REAL-SIZE CALCULATION OF HIGH-PRESSURE HYDROGEN FLOW AND AUTO-IGNITION IN CYLINDRICAL TUBE

Makoto ASAHARA, Akinori YOKOYAMA, Yuito TATSUMI,
Suguru KATO, Eisuke YAMADA, A. Koichi HAYASHI

Department of Mechanical Engineering, Aoyama Gakuin University
5-10-1 Fuchinobe, Chuo, Sagamihara, Kanagawa 252-5258, Japan

ABSTRACT

A real-size calculation is performed for high-pressure hydrogen release in a tube using the axisymmetric Navier–Stokes equations with the full hydrogen chemistry. A Harten–Yee-type total variation diminishing scheme and point-implicit method are used to integrate the governing equations. The calculated real-size results show that the leading shock wave velocity is similar to that calculated using a smaller tube. The mixing process and ignition behavior of high-pressure hydrogen are explained in detail; the velocity shear layer and Kelvin–Helmholtz instability are the main causes of mixing of hydrogen with air and ignition in the high-temperature region behind the leading shock wave.

1. Introduction

The behavior and ignition characteristics of spilled hydrogen must be understood in order to handle high-pressure hydrogen at hydrogen stations. Under current safety provisions, when pressure in a hydrogen vessel becomes extremely high, hydrogen is released through a safety valve to reduce the vessel pressure. However, spilled high-pressure hydrogen reportedly ignites without any ignition source when it goes through a pipe.

Wolański and Wójcicki [1] presented the first hydrogen auto-ignition study. Their analysis indicated that the ignition reaction started in the local high-temperature region behind a shock wave developed by high-pressure hydrogen when the shock wave emerged from a tube. In the context of developing a safety standard, Dryer et al. [2] showed that auto-ignition was caused by local reflected shock waves resulting from differences in the tube area. Golub et al. [3] and Mogi et al. [4] performed experimental works on hydrogen auto-ignition occurring in the atmosphere when high-pressure hydrogen spurted out of a tube. They found that auto-ignition is related to the tube size, with auto-ignition occurring at low pressure when tube length is longer. However, Kitabayashi et al. [5] recently showed experimentally that auto-ignition occurs again at higher pressure when the tube diameter increases. This finding may be attributed to wall friction in the tube. On the other hand, Xu et al. [6] demonstrated by their numerical work that a combustible mixture is produced at the contact

area between hydrogen and air, and that when the tube is long enough, auto-ignition starts in the tube, and the tube length plays an important role in producing mixing in the tube. Most recently, Kim et al. [7] presented experimental work showing that auto-ignition occurs near the wall just behind the precursor shock wave. They used a transparent tube to see the ignition point in the tube. However, even using the transparent tube, it is difficult to recognize the mechanism of high-pressure hydrogen auto-ignition in the tube.

The present study presents a real-size analysis of high-pressure hydrogen auto-ignition in a tube using the compressible Navier–Stokes equations with the full hydrogen reaction mechanism.

2. Numerical method

The governing equations are the compressible cylindrical Navier–Stokes equations (Eqs. 1 and 2) with a detailed reaction hydrogen–air reaction mechanism.

$$\frac{\partial Q}{\partial t}+\frac{\partial E}{\partial x}+\frac{\partial F}{\partial r}+G=\frac{\partial E_v}{\partial x}+\frac{\partial F_v}{\partial r}+G_v+S\,, \tag{1}$$

where

$$Q=\begin{pmatrix}\rho\\ \rho u\\ \rho v\\ e\\ \rho_i\end{pmatrix},E=\begin{pmatrix}\rho u\\ p+\rho u^2\\ \rho uv\\ (e+p)u\\ \rho_i u\end{pmatrix},F=\begin{pmatrix}\rho v\\ \rho vu\\ p+\rho v^2\\ (e+p)v\\ \rho_i v\end{pmatrix},G=\begin{pmatrix}\rho v/r\\ \rho uv/r\\ \rho v^2/r\\ (e+p)v/r\\ \rho_i v/r\end{pmatrix}$$

$$E_v=\begin{pmatrix}0\\ \tau_{xx}\\ \tau_{xr}\\ \tau_{xx}u+\tau_{xr}v-q_x\\ \rho D_i\dfrac{\partial Y_i}{\partial x}\end{pmatrix},F_v=\begin{pmatrix}0\\ \tau_{rx}\\ \tau_{rr}\\ \tau_{rx}u+\tau_{rr}v-q_r\\ \rho D_i\dfrac{\partial Y_i}{\partial r}\end{pmatrix},G_r=\begin{pmatrix}0\\ \tau_{rx}/r\\ \tau_{rr}/r\\ (\tau_{rx}u+\tau_{rr}v-q_r)/r\\ \rho_i v/r\end{pmatrix},S=\begin{pmatrix}0\\ 0\\ 0\\ 0\\ \dot{\omega}_i\end{pmatrix}$$

and

$$\tau_{xr}=\tau_{rx}=\mu(u_r+v_x),\tau_{xx}=\frac{2}{3}\mu(2u_x-v_r),\tau_{rr}=\frac{2}{3}\mu(2v_r-u_x)\,. \tag{2}$$

The equations are integrated explicitly and two-dimensionally in the radial and axial directions by the finite difference method: a Harten–Yee, second-order explicit non-MUSCL modified-flux-type total variation diminishing scheme [8] for the convective terms, a point-implicit method for the production terms, a central difference scheme for the diffusion terms, and a second-order Strang-type fractional step method for the unsteady term. A Petersen–Hanson model [9] is used for the chemical

reaction system, which has 9 species, H_2, O_2, O, H, OH, HO_2, H_2O_2, H_2O, and N_2, and 18 elementary reactions, and is developed to consider the effect of high-pressure and high-temperature conditions. The diffusion coefficient developed by Chapman and Cowling (Eq. 3) [10], the molecular viscous coefficients of Chapman and Enskog (Eq. 7) [11] and Wilke's law (Eq. 9) [12] are applied to calculate the transport coefficients as follows:

$$D_{ij} = 1.8829\times10^{-2}\frac{\sqrt{T^3 m_{ij}}}{p\sigma_{ij}^2\Omega_D}, \tag{3}$$

where m is the molar reduced mass, $\neg_{ij}$ is the collision diameter, and $\rightleftharpoons_D$ is the diffusion collision integral:

$$m_{ij} = \frac{m_i m_j}{m_i + m_j}, \tag{4}$$

$$\sigma_{ij} = \frac{1}{2}\left(\sigma_i + \sigma_j\right), \tag{5}$$

$$\Omega_D = \left(\frac{T}{T_{\varepsilon ij}}\right)^{-0.145} + \left(\frac{T}{T_{\varepsilon ij}+0.5}\right)^{-2.0}, \tag{6}$$

and

$$\mu_i = 2.6693\times10^{-6}\frac{\sqrt{W_i T}}{\sigma_i^2\Omega_v}, \tag{7}$$

where $\Omega_v = 1.147\times\left(\frac{T}{T_{\varepsilon ij}}\right)^{-0.145} + \left(\frac{T}{T_{\varepsilon ij}}+0.5\right)^{-2.0}$ (8)

and

$$\mu = \sum_{i=1}^{N}\frac{\mu_i}{1+\sum_{j\neq1}\varphi_{ij}\frac{X_j}{X_i}}, \tag{9}$$

where $\varphi_{ij} = \frac{\left[1+\left\{\left(\mu_i/\mu_j\right)\left(\rho_j/\rho_i\right)\right\}^{1/2}\left(W_i/W_j\right)^{1/4}\right]^2}{2\sqrt{2}\left\{1+\left(W_i/W_j\right)\right\}^{1/2}}$. (10)

The thermal conductivity $\asymp$ is obtained from the Wassiljewa equation (Eq. 11) [13] and the Eucken correction $\asymp_{ij}$ (Eq. 12) [14] as follows:

$$\kappa = \sum_{i=1}^{N} \frac{\kappa_i}{1 + \sum_{j \neq 1} \psi_{ij} \frac{X_j}{X_i}}, \quad \psi_{ij} = 1.065 \varphi_{ij} \tag{11}$$

and

$$\kappa_i = \kappa_i^{trans} + \kappa_i^{int} = \left(\frac{5}{2} C_{ci}^{trans} + C_i^{int} \right) \mu_i = \frac{1}{4} (9\gamma - 5) \mu_i C_{vi}, \tag{12}$$

where $\gamma = C_{pi} / C_{vi}$ *and* $C_{vi} = C_{pi} - R_i$.

The bulk viscosity, the Soret effect, the Dufour effect, pressure gradient diffusion, and gravity are neglected in the present analyses. The boundary conditions are (i) the left boundary is the inlet, (ii) the wall conditions are adiabatic, and (iii) the upper boundary is axisymmetric. The initial condition is that the computed area contains standard air and high-pressure hydrogen spurted into the tube at time zero.

3. Numerical results and discussion

The numerical results show the real size of the high-pressure hydrogen auto-ignition problem as follows: (i) a comparison of the present numerical results with experimental ones in terms of the relation between the burst pressure and shock wave velocity, (ii) the effect of the burst pressure on the physical values' history, and (iii) the hydrogen propagation and ignition behavior.

3.1 Comparison of present numerical results with experimental ones in terms of the relation between burst pressure and shock wave velocity

The relationship between the mean shock speed c_s and the burst pressure can be obtained theoretically to the first order using the equation derived from the shock wave relation. We compared the present numerical results and experimental ones. The experimental results using relatively short tubes (e.g., 300 mm and 650 mm) yield a velocity of 100–200 m/s, which differs from the theoretical results, as shown in Fig. 1. However, the theory provides results similar to those experimentally obtained by Mogi et al. [4], who used a tube with an electric valve to produce a high-pressure hydrogen jet. For tube lengths of 2.2–2.3 m, the shock wave speed becomes 300–400 m/s lower than the theoretical one because of viscous interactions with the tube wall and vortices. The results of experiments with a short tube are obviously closer to the theoretical ones. From these results, we may say that the longer tube has these kinematic losses.

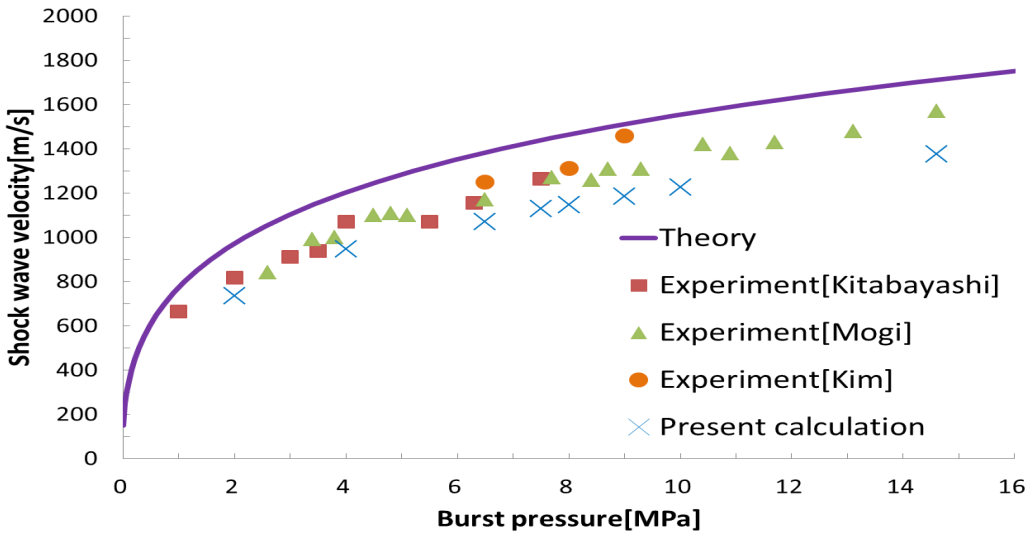

Fig. 1 Comparison of present numerical results with experimental data: relation between burst pressure and shock wave velocities.

3.2 Effect of burst pressure on physical values' history

Past experiments have shown that auto-ignition at the exit of the tube depends on the burst pressure and occurs at higher burst pressures. Here we studied the relation between the maximum temperature and OH mass fraction and the burst pressure by keeping the tube length constant. The results showed that auto-ignition at the tube exit did not occur at a burst pressure of 4.0 MPa, blow-off happened at 6.5 MPa, and auto-ignition occurred at 10.0 MPa. Figure 2 shows the maximum temperature history at the contact surface between hydrogen and air [Fig. 2-(a)] and the OH mass fraction history in vortices behind the contact surface [Fig. 2-(b)] in the tube. Figure 2-(a) shows that at three different burst pressures, the maximum temperature exceeds 3000 K after high-pressure hydrogen enters the tube. In these cases, the temperature becomes higher as the burst pressure increases and then decreases until 50 μs later. However, the maximum temperature does not decrease greatly, and the maximum OH mass fraction retains its value of 0.012, which is quite high and implies that the reaction is proceeding. From these results we can say that the reaction occurs in the tube.

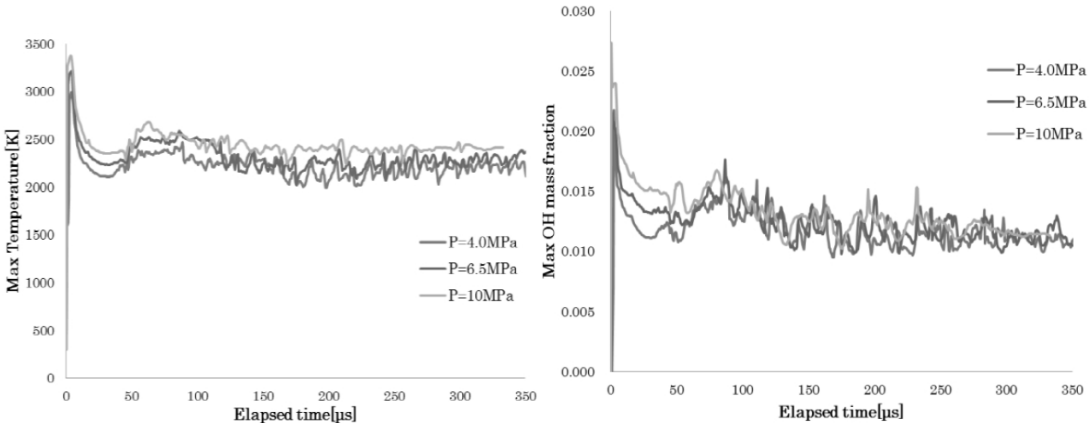

(a) Maximum temperature history (b) Maximum OH mass fraction history

Fig. 2 Time histories of maximum temperature and OH mass fraction in the tube.

3.3 Hydrogen propagation and ignition behavior

Here we discuss the mixing of hydrogen and air and their ignition process at a burst pressure of 14.6 MPa. Figure 3 shows time sequences of the temperature profiles near the contact surface between high-pressure hydrogen and air. Air is on the right side of the figure, and the leading shock wave caused by the high-pressure hydrogen propagates from left to right. The contact surface between hydrogen and air exists behind the leading shock wave, and the region between the leading shock wave and the contact surface is a mixing zone of hydrogen and air. It can be seen that the hydrogen temperature exceeds the hydrogen ignition temperature of 843 K, and the reaction occurs at the contact surface between 2.63 and 14.0 ㎲s. However, the reaction zone is not growing at these times because mixing is not strong enough. After 19.7 ㎲s, the contact surface becomes irregular owing to Kelvin–Helmholtz instability behind the contact surface.

Regarding vortex production behind the contact surface, which may be the cause of auto-ignition in the tube, Fig. 4 shows the temperature contours at 14.0 ㎲s, where Fig. 4-(a) shows the temperature contours of the entire numerical field, and Fig. 4-(b) shows the local temperature profiles of one region in Fig. 4-(a). It is understood from Fig. 4-(b) that the temperature on the contact surface is high, and a discontinuous line appears behind the contact surface, which implies that the ignition and instability emerge there. Figure 5 shows the *y*-direction velocity profiles behind the contact surface. The large *y*-direction velocity implies the existence of large velocity differences and the resulting vortices. The vortices originate in the velocity shear layer because of Kelvin–Helmholtz instability.

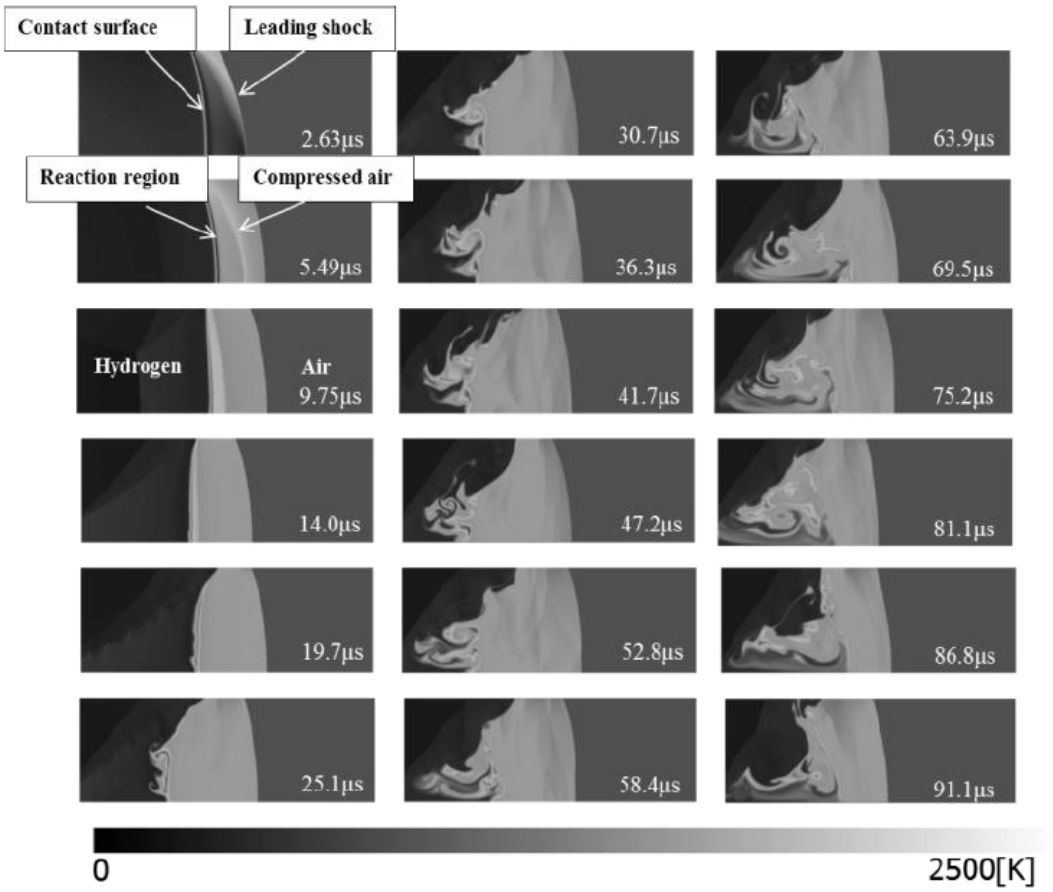

Fig. 3 Time histories of temperature profiles in the tube at burst pressure of 14.6 MPa.

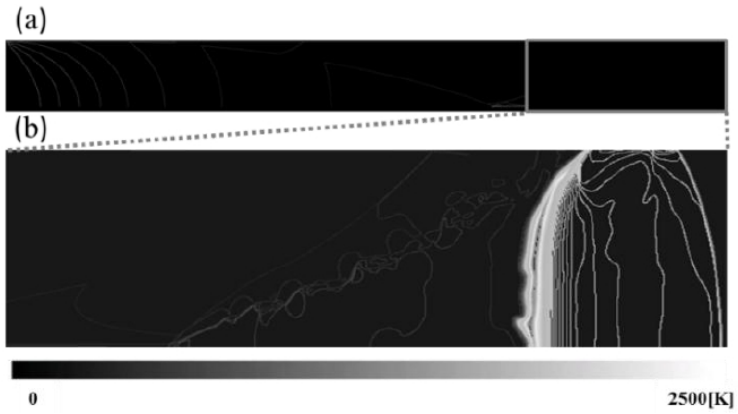

Fig. 4 Detailed temperature contours at 14.0 ms: (a) temperature profiles of entire numerical field and (b) local temperature profiles of one region in Fig. 4-(a).

Fig. 5 *y*-direction velocity profiles for burst pressure of 14.6 MPa at 14.0 ms.

4. Conclusions

Real-size high-pressure hydrogen release in a tube was numerically studied, yielding the following results.

(1) The real-size calculation shows results similar to those of small-size calculations: ignition occurs inside the tube, although it is not seen at the exit of the tube. In this case, ignition in the tube might be blown off at the exit of the tube.

(2) The chemical reaction in the tube is maintained by mixing between hydrogen and air by the vortices produced by Kelvin–Helmholtz instability in the tube.

References

1. Wolański, P., Wójcicki, S., “Investigation into the mechanism of the diffusion ignition of a combustible gas flowing into an oxidizing atmosphere,” Proc. Combust. Inst. 14 (1972) 1217–1223.
2. Dryer, F.L., Chaos, M., Zhao, Z., Stein, J.N., Alpert, J.Y., Homer, C.J., “Spontaneous ignition of pressurized release of hydrogen and natural gas into air,” Combust. Sci. Technol., Vol. 179, Issue 4–6, April (2007) 663–694.
3. Golub, V.V., Baklanov, D.L., Bazhenova, T.V., Bragin, M.V., Glovastov, S.V., Ivanov, M.F., Volodin, V.V., “Shock-induced ignition of hydrogen gas during accidental or technical opening of high-pressure tanks,” J. Loss Prev. Process Ind., Vol. 20, Issues 4–6, July-November (2007) 439–446.
4. Mogi, T., Wada, Y., Ogata, Y., Hayashi, A.K., “Self-ignition and flame propagation of high pressure hydrogen jets during sudden discharge from a pipe,” Int. J. Hydrogen Energy, Vol. 34, Issue 14, July (2009) 5810–5816.
5. Kitabayashi, N., Wada, Y., Mogi, T., Saburi, T., Hayashi, A.K., “Experimental study on high pressure hydrogen jets coming out of tubes of 0.1-4.2 m in length,” Int. J. Hydrogen Energy, Vol. 39, Issue 19 (2012) 8100–8107.

6. Xu, B.P., Wen, J.X., Dembele, S., Tam, V.H.Y., Hauksworth, S.J., “The effect of pressure boundary rupture rate on spontaneous ignition of pressurized hydrogen release,” J. Loss Prev. Process Ind., Vol. 22 (2009) 279–287.
7. Kim, Y.R., Lee, H.J., Kim, S., Jeung, In-S., “A flow visualization study on self-ignition of high pressure hydrogen gas released into a tube,” Proc. Combust. Inst., Vol. 34, Issue 2 (2013) 2057–2064.
8. Yee, H.C., “Upwind and Symmetric Shock-Capturing Scheme,” NASA Technical Memorandum, 89464, 1987.
9. Petersen, E.L., Davidson, D.F., Hanson, R.K., “Reduced kinetics mechanism for ram accelerator combustion,” J. Propul. Power, Vol. 15, Issue 4 (1999) 591–600.
10. Chapman, S., Cowling, T.G., “The Mathematical Theory of Non-Uniform Gases,” Cambridge University Press, UK, 1970.
11. Bird, R.B., Stewart, W.E., Lightfoot, E.N., “Transport Phenomena,” Wiley, 1960.
12. Wilke, C.R., “A viscosity equation for gas mixtures,” J. Chem. Phys., Vol. 18, Issue 4 (1950) 517–519.
13. Wassiljewa, A., “Wärmeletiung in Gasgemischen,” Physik. Z., Vol. 5 (1904) 737–742.
14. Eucken, A., “Über das Wärmeleitvermögen, die spezifische Wärme und die innere Reibung der Gase,” Phys. Z., Vol. 14 (1913) 324–332.